ERJ
Engineering Research Journal
Faculty of Engineering
Menoufia University

MAXIMUM TORQUE / AMPERE OF POSITION SENSORLESS CONTROL OF SYNCHRONOUS RELUCTANCE MOTOR

Z.M.S. Elbarbary ,
Faculty of Engineering - KFS University

Abstract

This paper introduced maximum torque per ampere of position sensorless control of Three-phase synchronous reluctance motor drive system. The proposed system is based on indirect rotor field oriented control . The rotor position is estimated using the active flux observer method . The drive system is investigated at different operating conditions. The proposed system is robust and suitable for high performance three-phase synchronous reluctance motor drives. Simulation is carried out by using the Matlab/Simulink package. The results validate the proposed approaches.

الملخص العربي

يقدم هذا البحث نظام تسيير محرك محرك الاعاقه ثلاثى الاوجه . يعتمد هذا النظام على نظرية التوجيه الغير مباشر للمجال معتمدا على استشعار الزاويه وتحقيق اقصى عزم / أمبير ويقدم البحث التحليل الرياضي والمحاكاة للطريقة المقترحة لنظام التحكم ذي المسار المغلق لمحركات الاعاقه المتزامنه ثلاثية الاوجه وذلك لبحث خصائص أدائها مقترنة بهذه الطريقة، ويقدم البحث عرضا للنتائج عند حالات التشغيل المختلفة. وقد اثبتت النتائج قوة نظام التحكم المقترح كما انه يعطى خصائص اداء عاليه لتسيير محركات الاعاقه المتزامنه ثلاثية الاوجه.

Keywords: Synchronous reluctance motor, position sensorless control, field oriented control

Nomenclature

V : Stator voltage
R_s : stator phase resistance (ohm)
d,q : direct and quadrature stator axis
L_d, L_q : direct and quadrature axis inductances (H)
T_l : load torque (N.m)
J : inertia of motor ($Kg.m^2$)
B : friction coefficient (N.m.s/rad)
α : component along the stationary α –axis
β : component along the stationary β –axis
λ : Flux linkage

1. Introduction

The synchronous reluctance motor has many advantages such as simple and rugged structure with low manufacturing cost, absence of rotor winding, cold rotor due to reduced iron losses, reasonable efficiency and ability to operate in high speed application with high temperature environment, In addition, there is no slip frequency between the stator and rotor for the SynRM as it is with the synchronous reluctance motor. svgg. To improve the reliability and dynamic performance of the SynRM drive system, sensorless rotor position estimating techniques have been proposed to eliminate the rotor position sensor . Where many research have been done to improve the performance of the sensorless based drive.

The main advantage of free predictive current control for synchronous reluctance motor (SynRM) drives are that it does not require specific SynRM models and it requires neither motor parameters nor back-EMF estimations. However, this approach has two disadvantages: 1) two current measurements are required in each sampling period, which may lead to detection of undesirable current spikes caused by instantaneous switching inside the inverter, and 2) an unresolved problem of stagnant current-variation updates, which undermines prediction performance. In [1] the author intends to eliminate these two drawbacks. In [2], a hybrid motion sensorless control of an axially laminated anisotropic reluctance synchronous machine (RSM). The zero- and low-speed sensorless method is a saliency-based high-frequency signal injection technique that uses the motor itself as a resolver. The second method is based on a state observer incorporating the active-flux" concept used to deliver RSM rotor position and speed information for medium and high-speed range. In [3], The estimation of speed and rotor angle is based on extended programmable cascaded low-pass filters (LPFs), which effectively reduce the effects of direct-current (dc) offsets at low speeds. The effect of the number of LPF stages on output dc offset, estimation accuracy, and dynamic performance are investigated, and their equations are developed. In [4], A digital strategy to suppress magnetic- and cross-saturation effects in a sensorless predictive direct-torque-controlled synchronous reluctance machine is introduced. However, magnetic- and cross-saturation effects lead to large errors on the estimated angular position, particularly when the magnetization level and torque load change. The saturation effects can be

readily alleviated by using a digitally implemented quadratur phase-locked loop observer, together with linear regression. In [5] a high-frequency injection method used to estimate rotor position taking into account the influence of the rotor speed during the estimation interval to reduce the rotor position estimation error. In [6], The active-flux (AF) and arbitrary injection position estimation techniques are combined for the first time in this hybrid controller. A hysteresis region is implemented with phase-locked loop synchronization for dynamic and stable change over between estimators. In [7] The control system is based on the active flux concept and a hybrid rotor position estimation algorithm is used, being this algorithm based on the injection of high frequency signals at low speeds and on the position of the active flux vector for medium and high-speeds. A smooth transition algorithm between the two rotor position estimation methods is provided. To improve the efficiency of the overall drive system, a loss minimization algorithm is introduced. In this paper the rotor position estimation using active flux observer together with field oriented control is presented and analyzed, from the control's point of view, engaging the maximum

torque per ampere (MTPA) strategy on a simulated machine model. The actual simulation model is designed in Matlab /Simulink, containing the machine and its control unit.The present analysis does not take into account the iron losses and the saturation.

2. Vector Control of 3-Phase Synchronous Motor

The theory of indirect field oriented control is applied for the Three-phase synchronous reluctance motor. The application of the vector control scheme to such arrangement is simple, and can provide fast-decoupled control of torque and flux. Figure 1 shows the overall block diagram of the drive system. When a set value for the speed is fed into the speed loop, the signal will be regulated using the PI controller as adaptive mechanism, results in the q-axis current I_q^* which is equal to I_d* according to maximum torque per ampere strategy [12-20]. Both The two current command components are then transformed with the help of rotor position angle (θ_r) to Three current commands i_a, i_b and i_c in the stationary reference frame. These current commands are then compared to the actual motor currents by hysteresis current controller to generate the logic pulses for the inverter switches. In Fig.1, the motor speed ω_r is compared to a command speed, ω^*,
and the error signal is processed by the PI controller, to generate the torque-component current command I_q^* as follow:

$$T_e^* = (\omega_r^* - \omega_r)\frac{K_{ps}\,[1+\tau_{cs}S]}{\tau_{cs}S} \quad (1)$$

$$I_{sq}^* = \sqrt{\frac{T_e^*}{\frac{3}{2}\frac{P}{2}(L_{sd}-L_{sq})}} \quad (2)$$

And, for ideal condition, of maximum per ampere torque, keeping dq- current components equal, i.e. ($I_{sqm}^* = I_{sdm}^*$) , this happened at angle 45^0 as shown in figure (1):

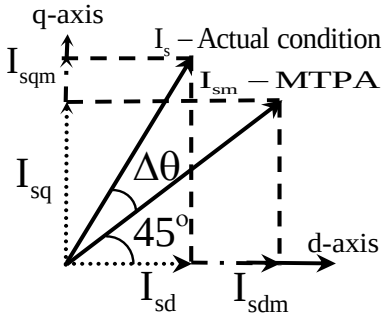

Figure (1) phasor diagram of MTPA operation

Due to the iron losses of the motor the current is shifted by($\Delta\theta$) from the maximum torque position.

The transformations from rotating reference frame (dq-axis) to stationary frame (α-β axis) used for the present work are expressed as follows;

$$qd/\alpha\beta = \begin{Bmatrix} i_\alpha^* = i_q^*\cos\theta_r + i_d^*\sin\theta_r \\ i_\beta^* = -i_q^*\sin\theta_r + i_d^*\cos\theta_r \end{Bmatrix} \quad (3)$$

Where θ_r represents the rotor angle.

$$\alpha\beta \rightarrow abc = \begin{bmatrix} 1 & 0 \\ \frac{-1}{2} & \frac{\sqrt{3}}{2} \\ \frac{-1}{2} & \frac{-\sqrt{3}}{2} \end{bmatrix} \begin{bmatrix} i_\alpha \\ i_\beta \end{bmatrix} \quad (4)$$

And the inverse from three phase to αβ axis is:

$$abc \rightarrow \alpha\beta = \begin{bmatrix} 1 & 0 & 1 \\ \frac{-1}{2} & \frac{\sqrt{3}}{2} & 1 \end{bmatrix} \begin{bmatrix} i_a \\ i_b \\ i_c \end{bmatrix} \quad (5)$$

The above three phase reference currents are compared with the actual three phase motor currents

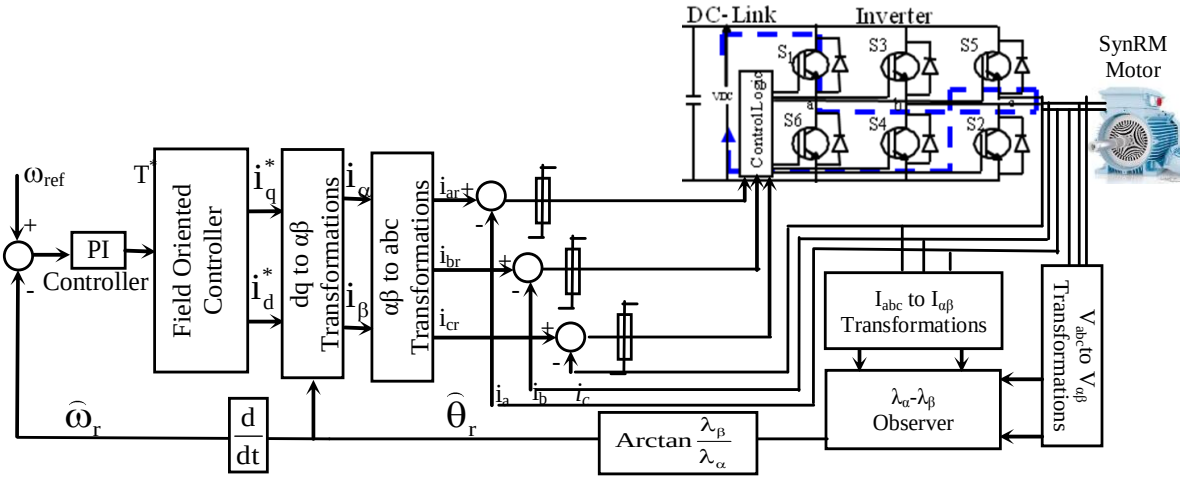

Fig. (2) Block diagram of the proposed position sensorless control system

switching logic of the three phase inverter. The modulated phase voltages of Three-phase inverter are introduced as a function of switching logic NA, NB and NC of power switches by the following relations:

$$\begin{bmatrix} V_a \\ V_b \\ V_c \end{bmatrix} = \frac{V_{dc}}{3} \begin{bmatrix} 2 & -1 & -1 \\ -1 & 2 & -1 \\ -1 & -1 & 2 \end{bmatrix} \begin{bmatrix} NA \\ NB \\ NC \end{bmatrix} \quad (6)$$

The per-phase switching state having a range of N = 0 or 1.

3. Mathematical Model of Synchronous Reluctance Motor

The dynamic model of the motor in rotating reference frame can be represented as follow:

$$V_q = R_s i_q + \frac{d\lambda_q}{dt} + p\omega_r \lambda_d \quad (7)$$

$$V_d = R_s i_d + \frac{d\lambda_d}{dt} - p\omega_r \lambda_d \quad (8)$$

The stator q and d-axis flux linkage is given by:

$$\lambda_q = L_q i_q$$
$$\lambda_d = L_d i_d \quad (9)$$

The electromagnetic torque is given by:

$$T_e = -\frac{p}{2}(\lambda_q i_d - \lambda_d i_q) \quad (10)$$

$$\frac{d\omega}{dt} = \frac{1}{J}(T_e - T_l - B\omega) \quad (11)$$

4. ACTIVE FLUX BASED POSITION AND SPEED ESTIMATING METHOD

From the SynRM stator voltage vector equation,

$$\overrightarrow{V_s} = R_s \overrightarrow{i_s} + \frac{d\vec{\lambda}_s}{dt} \quad (12)$$

We can obtain, the stator flux vector as follow :

$$\overrightarrow{\lambda_s} = \int (\overrightarrow{V_s} - R_s \overrightarrow{i_s}) dt \quad (13)$$

And the active stator flux component are obtained as follow:

$$\overrightarrow{\lambda_\alpha} = \int (\overrightarrow{V_\alpha} - R_s \overrightarrow{i_\alpha}) dt - L_q i_\alpha \quad (14)$$

$$\overrightarrow{\lambda_\beta} = \int (\overrightarrow{V_\beta} - R_s \overrightarrow{i_\beta}) dt - L_q i_\beta \quad (15)$$

Where, λ_α, λ_β, are the α and β-axis components of the stator flux .

The Estimated rotor position angle $\hat{\theta}_r$ is,

$$\hat{\theta} = \arctan \frac{\int (\overrightarrow{V_\beta} - R_s \overrightarrow{i_\beta}) dt - L_q i_\beta}{\int (\overrightarrow{V_\alpha} - R_s \overrightarrow{i_\alpha}) dt - L_q i_\alpha} \quad (16)$$

And the estimated rotor speed is $\hat{\omega}_r = \frac{d\hat{\theta}_r}{dt}$ (7)

From the above two equations, the only problem of the position and speed estimation algorithm may comes from the integration. This method is simple in calculation and has a fast response.

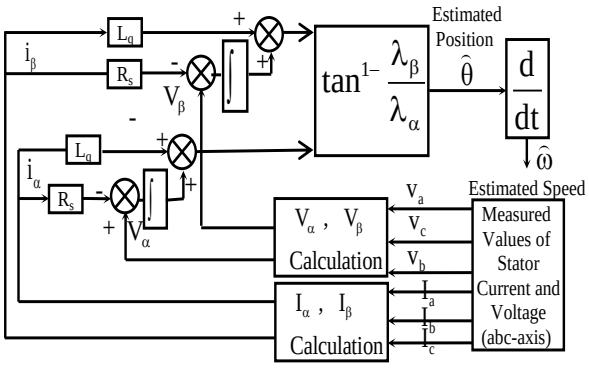

Fig. (3) Position and speed estimation based AFO.

5. SIMULATION RESULTS

The proposed control system shown in Figure 2 is designed for a simulation investigation with aid of figure 3. Simulation is carried out using the general purpose simulation package Matlab/Simulink [21], Simulation results are presented to show the effectiveness of the proposed scheme at different operating conditions. These results are classified into two categories; the first represents startup and steady-state while the second represents the dynamic performance

5.1. Starting and Steady-State Performance

The simulation result for start-up and steady-state performance is illustrated by Figs. 4 to 6. Figure 4.a shows the variation of motor speed from startup to the steady state speed (300 rad/sec), which is reached after about 100 m sec. dq axis current components are shown in figure 4b, as seen the two component are overlapped The developed torque and motor current corresponding to same period are shown in Figs. 4.c and 4.d respectively. These current signals are of sine wave profiles on which controller transients are shown figure 4e shows the rotor angle, estimated from the observer and measured, as seen, the two signals are correlated.

5.2. Dynamic Performance

For studying the dynamic performances of the proposed system, simulation has been carried out. In this respect, the dynamic response of the proposed algorithm is examined by step changes for both speed reference and load torque.

5.2.1. Speed Step Change

To study the dynamic response of the control system due to a step change in the speed command, the motor is subjected to a step increase and decrease in the speed command to evaluate its performance. Figure.5a shows the variation of motor speed, which at t=0.5 second the motor speed command is changed from 200 rad/sec to 350 rad/sec. and return back again after one second. It can be seen that the motor speed is accelerated and decelerated smoothly to follow its reference value with nearly zero steady state error. Figures 5.b and 5.c show the developed torque and motor current corresponding to this step changes respectively. These results ensure the effectiveness of the proposed controller and show good behavior of its dynamic response.

5.2.2. Load Step Change

The ability to withstand disturbances in IM control system is another important feature. A step change in the motor load is considered as a typical disturbance. A high performance control system has fast dynamic response in adjusting its control variables so that, the system outputs affected by the load impact will recover to the original status as soon as possible. The dropped aptitude of the system output such as rotor speed and its recovering time are the important performance specifications. Figure 6a shows the speed response when a load impact is applied for one second. The motor started at no load and the load of (5 N.m), is applied for one second. The corresponding developed torque is shown in Fig6b. Fig.6c show motor phase current, which increases with loading and decreases with load release.

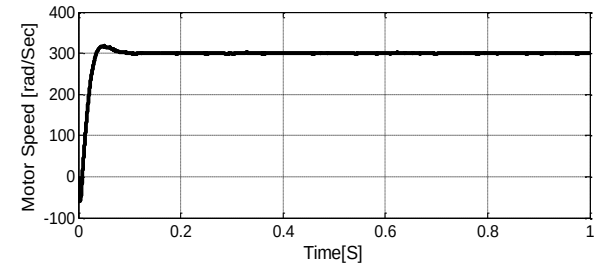

(a)

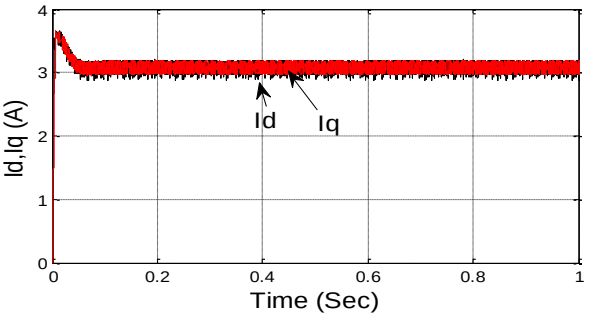

(b)

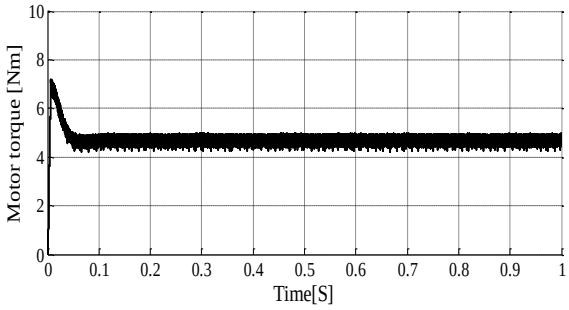

(c)

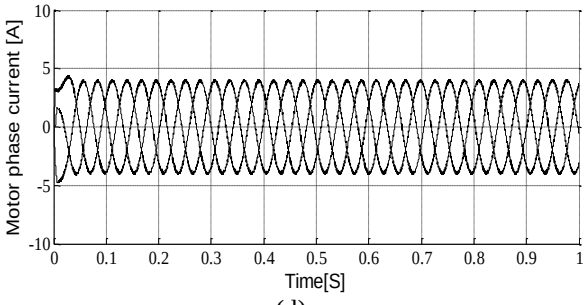

(d)

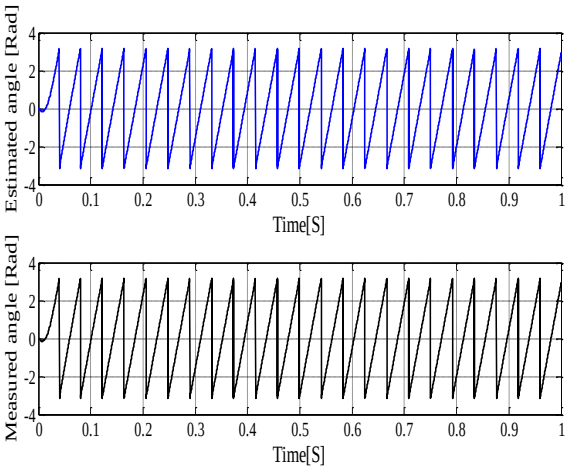

(e)

Fig.4 Startup and steady-stat performance, a-motor speed b- Id and Iq currents c- motor torque d-three phase motor current d- motor angle, estimated and measured

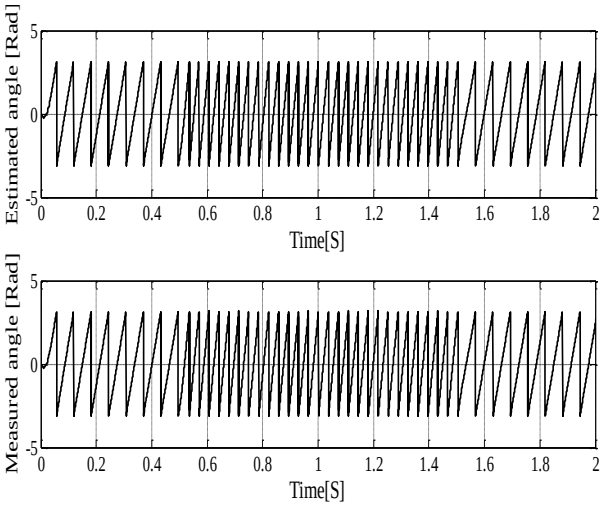

(e)

Fig.5 Speed step up and down changes, a-motor speed b- Id and Iq currents c- motor torque d-three phase motor current d- motor angle, estimated and measured

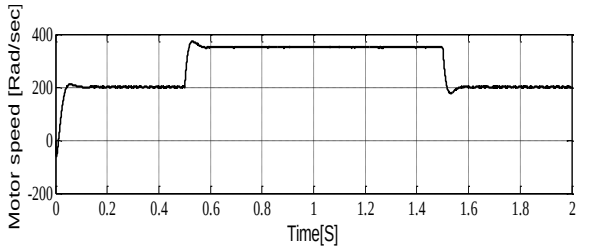

(a)

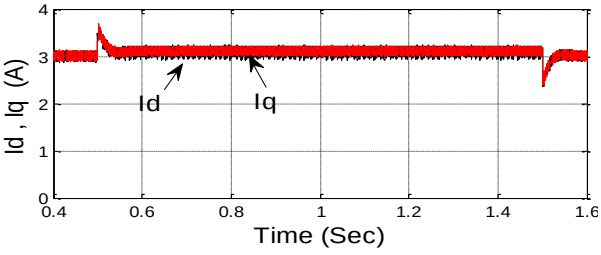

(b)

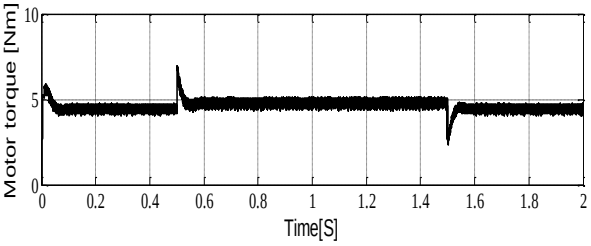

(c)

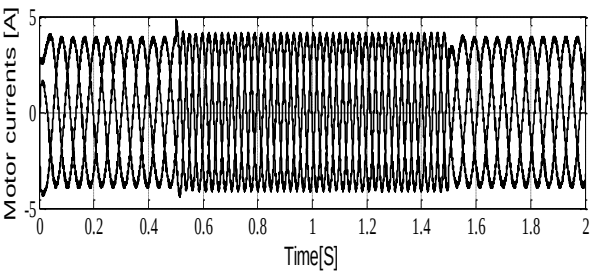

(d)

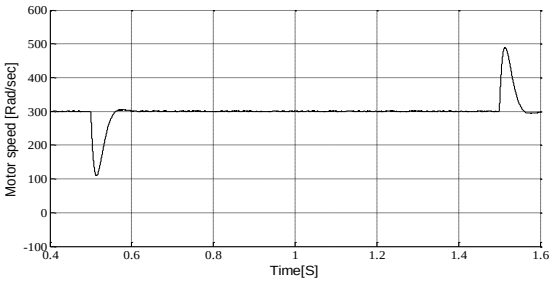

(a)

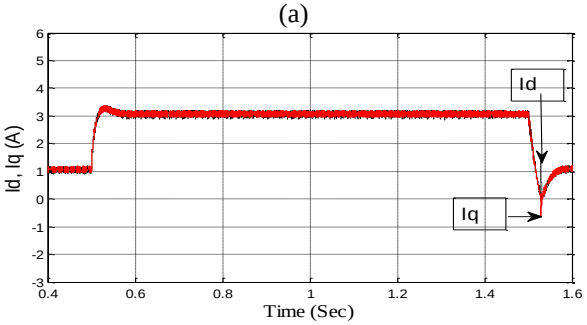

(b)

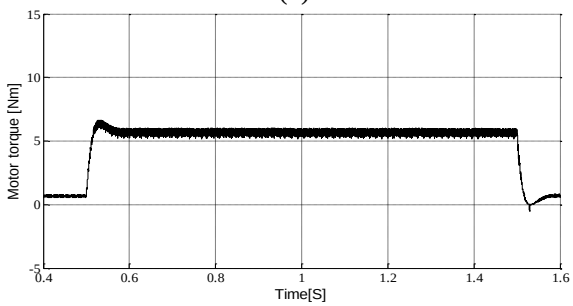

(c)

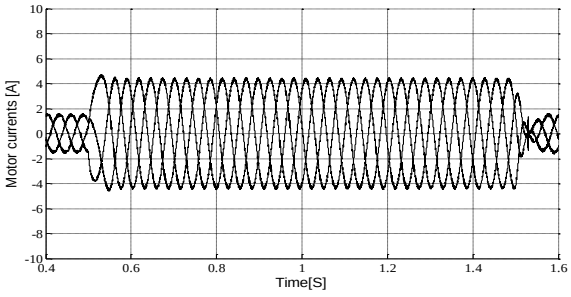

(d)

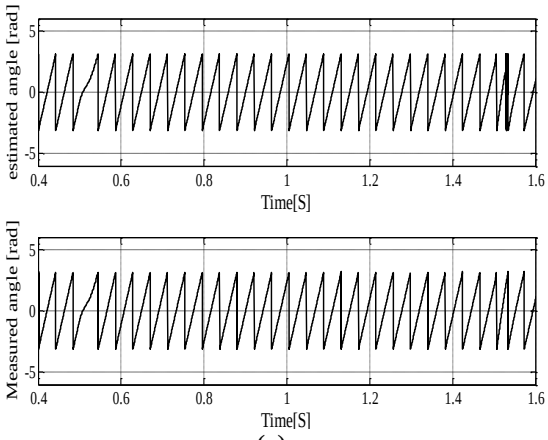

(e)

Fig.6 Load impact, a-motor speed b- Id and Iq currents c- motor torque d-three phase motor current d- motor angle, estimated and measured

6. Conclusion:

This paper presents a position seensorless control of Three-phase synchronous reluctance motor. accomplished with maximum torque per ampere control method. As seen, the best control point is reached where the D and Q currents are equal. This condition is reached when the angle between them is 45deg. The advantage of this method is that the losses are minimum because the most important losses in a machine are those in the windings. As seen in the results of the simulations, the two currents overlap at any moment of operation in the machine. The machine was tested at rated speed, and the torque was varied from 0 to the rated value of 5Nm. The behavior of the machine is satisfactory for the entire range of torque values. Future studies will include consideration of the losses and saturation effects in the machine model.

7. References

[1] Levi, E., Bojoi, R., Profumo, F., Toliyat, H.A., and Williamson, S., "Multiphase synchronous reluctance motor drives technology status review"' IEE Elec. Power appl., 2007.

[2] Cheng-Kai Lin; Jen-te Yu; Yen-Shin Lai; Hsing-Cheng Yu "Improved Model-Free Predictive Current Control for Synchronous Reluctance Motor Drives"IEEE Transactions on Industrial Electronics ,Year: 2016, Volume: 63, Issue: 6,Pages: 3942 - 3953,

[3] Sorin-Cristian Agarlita; Ion Boldea; Frede Blaabjerg"High-Frequency-Injection-Assisted "Active-Flux"-Based Sensorless Vector Control of Reluctance Synchronous Motors, With Experiments From Zero Speed "IEEE Transactions on Industry Applications Year: 2012, Volume: 48, Issue: 6 ,Pages: 1931 - 1939,

[4] Ahmad Ghaderi; Tsuyoshi Hanamoto"Wide-Speed-Range Sensorless Vector Control of Synchronous Reluctance Motors Based on Extended Programmable Cascaded Low-Pass Filters " IEEE Transactions on Industrial Electronics ,Year: 2011, Volume: 58, Issue: 6, Pages: 2322 - 2333,

[5] Roberto Morales-Caporal; Mario Pacas "Suppression of Saturation Effects in a Sensorless Predictive Controlled Synchronous Reluctance Machine Based on Voltage Space Phasor Injections "IEEE Transactions on Industrial Electronics ,Year: 2011, Volume: 58, Issue: 7,Pages: 2809 - 2817,

[6] Pin-Chia Pan; Tian-Hua Liu; Udaya K. Madawala "Adaptive controller with an improved high-frequency injection technique for sensorless synchronous reluctance drive systems" IET Electric Power Applications ,Year: 2016, Volume: 10, Issue: 4,Pages: 240 - 250,

[7] Francois J. W. Barnard; Wikus T. Villet; Maarten J. Kamper, " Hybrid active-flux and arbitrary injection position sensorless control of reluctance synchronous machines , 2014 International Symposium on Power Electronics, Electrical Drives, Automation and Motion Year: 2014 ,Pages: 1146 - 1151,

[8] Eva Serna Calvo; Detlef Potoradi, "Synchronous reluctance motors with and without permanent magnets for high performance low cost electrical drives", 5th International Electric Drives Production Conference (EDPC) ,Year: 2015 Pages: 1 - 7,

[9] Po-ngam, S.; Sangwongwanich, S., "Stability and

[10] Dynamic Performance Improvement of Adaptive Full-

[11] Order Observers for Sensorless PMSM Drive," IEEE

[12] Trans. Power. Electr., vol. 27, pp. 588 – 600, Feb. 2012

[13] Guglielmi, P., Pastorelli, M., Pellegrino, G., & Vagati, A. "Position sensorless control of permanent magnet assisted synchronous reluctance motors." Industry Applications Conference, 2003. 38th IAS Annual Meeting. Conference Record of the, 2, 933–939 vol.2.

[14] Tuovinen, T., Hinkkanen, M., Harnefors, L., & Luomi, J. (2012). Comparison of a reduced-order observer and a full-order observer for sensorless synchronous motor drives. IEEE Transactions on Industry Applications, 48(6), 1959–1967.

[15] Preindl, M., & Bolognani, S. Model predictive direct torque control with finite control set for PMSM drive systems, Part 1: Maximum torque per ampere operation. IEEE Transactions on Industrial Informatics, (2013),. 9(4), 1912–1921.

[16] Tu, X., & Gu, C. Maximum Torque per Ampere Control of Novel Transverse Flux Permanent Magnet Motor with Brushless DC Drive. PRZEGLAD ELEKTROTECHNICZNY(2012)., (4), 285–288.

[17] Daryabeigi, E., Abootorabi Zarchi, H., Arab Markadeh, G. R., Soltani, J., & Blaabjerg, FOnline MTPA control approach for synchronous reluctance motor drives based on emotional controller. IEEE Transactions on Power Electronics. (2015)., 30(4), 2157–2166.

[18] Antonello, R., Carraro, M., & Zigliotto, M.. Maximum-torque-per-ampere operation of anisotropic synchronous permanent-magnet motors based on extremum seeking control. IEEE Transactions on Industrial Electronics, 61(9), (2014), 5086–5093.

[19] Ruba, M., Jurca, F., Martis, C., Martis, R., & Piglesan, P. F. (2014). Analysis of maximum torque per ampere control strategy for variable reluctance synchronous machines for traction applications. In EPE 2014 - Proceedings of the 2014 International Conference and Exposition on Electrical and Power Engineering (pp. 322–326).

[20] Hrkel', M., Vittek, J., & Biel, Z. (2012). Maximum torque per ampere control strategy of induction motor with iron losses. In Proceedings of 9th International Conference, ELEKTRO 2012 (pp. 185–190).

[21] Consoli, a., Scarcella, G., Scelba, G., & Testa, a. (2010). Steady-State and Transient Operation of IPMSMs Under Maximum-Torque-per-Ampere Control. IEEE Transactions on Industry Applications, 46(1), 121–129.

[22] Itoh, J. I., Nakajima, Y., & Kato, M. (2013). Maximum torque per ampere control method for IPM Synchronous Motor based on V/f control. In Proceedings of the International Conference on Power Electronics and Drive Systems (pp. 1322–1327).

[23] Betz, R. E., Jovanovic, M., Lagerquist, R., & Miller, T. J. E. (1992). Aspects of the control of synchronous reluctance machines including saturation and iron losses. In Conference Record - IAS Annual Meeting (IEEE Industry Applications Society) (Vol. 1992–January, pp. 456–463).

[24] Matlab/Simulink Toolbox User's Guide, The Math works Inc., Natick, MA, USA, May 1998.

Appendix : Motor Parameter

No. of poles	4
Stator resistance	4 ohm
Frequency	50 Hz
Motor speed	1500 r.p.m.
Inertia	0.0006 kg.m2
DC- Link voltage (Vbus)	200 V;
Ld	0.6mH;
Lq	0.2mH;
B	0.009;